1   **Melanism in a wild sifaka population: Darker where cold and fragmented**

2   *Short title: Melanism in lemurs*

3   Elizabeth Tapanes[1], Jason M. Kamilar[2,3], Maanas A. Nukala[1], Mitchell T. Irwin[4,^], Brenda

4   J. Bradley[1,^]

5

6   [1] Center for the Advanced Study of Human Paleobiology, Department of Anthropology,

7   The George Washington University

8   [2] Graduate Program in Organismic and Evolutionary Biology, University of

9   Massachusetts Amherst

10   [3] Department of Anthropology, University of Massachusetts Amherst

11   [4] Department of Anthropology, Northern Illinois University

12

13   ^ = Should be considered co-senior authors

14

15   **Corresponding author:**

16   Elizabeth Tapanes

17   9500 Gilman Drive., Rm 2219

18   La Jolla, CA, 92161

19   Elizabeth.tapanes@gmail.com

20   (858) 534-6355

21

22   *Current affiliation for Elizabeth Tapanes: Department of Biological Sciences; Division of*

23   *Ecology, Behavior and Evolution, University of California San Diego*

Abstract

24

25   Pigmentation is one of the most striking examples of diversity in the natural world.

26   Mainly, pelage (hair/fur) pigmentation provides a substrate for selection (i.e., crypsis,

27   signaling, thermoregulation) and is capable of rapid change. Thus, this trait may be the

28   one potential early signal of adaptation (or maladaptation) in wild primate populations.

29   However, most of our hypotheses on the forces responsible for primate pelage

30   pigmentation are based solely on macro-evolutionary studies. Here, we characterize

31   pelage color and pattern variation within a population of wild primates, diademed sifakas

32   (*Propithecus diadema*), exhibiting striking diversity in coloration (melanic to tri-colored).

33   Our approach jointly assesses climate and pelage variation across the region. We score

34   pelage using a semi-quantitative methodology. We then test if pelage variation is

35   associated with climatic or demographic factors (i.e., sex-class, age-class) across the

36   Tsinjoarivo forest, Madagascar. We find darker bodies and less complex faces occur in

37   colder and more fragmented forests. We explore three hypotheses that may explain this

38   phenotypic pattern: isolation by distance, an environmental gradient, or unique local

39   adaptation. Importantly, each scenario signals the need for enhanced conservation of

40   diademed sifakas in the Tsinjoarivo forest. More studies on primate pigmentation in wild

41   populations will be needed to contextualize if this pattern is exceptional or typical. It is

42   likely that in other primate populations pigmentation may also foretell of adaptation or

43   environmental mismatch.

44   **Keywords:** ecological niche modeling, Indriidae, coloration, lemurs, trait evolution,

45   conservation

Introduction

Variation in pigmentation of pelage (hair, fur) exemplifies some of the most striking

observable diversity in mammals. Primates, in particular, exhibit some of the most

remarkable diversity in pelage pigmentation, displaying a high degree of inter- and

intraspecific variation (Bradley & Mundy, 2008; Caro et al., 2017). Pelage color patterns

span black and white variegated patterns (e.g., black-and-white ruffed lemur (*Varecia*

variegata)), orange hues (e.g., orangutans (*Pongo* spp.)), stripes (e.g., ring-tailed lemurs

(*Lemur catta*)), and intricate facial patterns (e.g., guenons (*Cercopithecus* spp.)) (Bradley

& Mundy, 2008). Current hypotheses argue that pelage pigmentation aids with crypsis,

signaling, and/or thermoregulation (Caro et al., 2021; Cuthill et al., 2017; Tapanes et al.,

2021). However, even against a backdrop of selection, neutral factors such as drift and

restricted gene flow can influence pigmentation patterns (Runemark et al., 2010).

Nevertheless, darker species tend to co-occur in warm, humid forests, and species with

more complex color patterns tend to live in larger groups or exhibit enhanced color vision

(Allen et al., 2014; Bell et al., 2021; Santana et al., 2012; 2013). These patterns may

implicate camouflage and crypsis, respectively. Additionally, many species exhibit

marked ontogenetic coat changes (Caro & Mallarino, 2020). However, most of what we

know about forces potentially driving variation in primate hair pigmentation derive from

macro-evolutionary studies across large portions of the order (e.g., all African monkeys

and apes) (Caro et al., 2021; Santana et al., 2013).

What drives variation on a micro-evolutionary scale is not always identical to

what drives macroevolutionary variation. For example, human hair color variation likely

evolved due to neutral forces such as drift—but, in general, variation across the primate

69   order exhibits evidence of potential adaptive evolution (Caro et al., 2021; Jablonski &

70   Chaplin, 2017; Santana et al., 2013; Tapanes et al., 2021). In both neutral and non-neutral

71   evolution, hair pigmentation is often capable of rapid change. When adaptive, variation in

72   hair within a population can mark the difference in an individual's survival or demise.

73   For example, snowshoe hare predation increases when a mismatch exists between coat

74   color and snow cover (Zimova et al., 2016). So, in response to milder winters in the

75   Pacific Northwest, hare populations are now rapidly evolving brown winter coats (Jones

76   et al., 2018). In primates, mantled howler monkey (*Alouatta palliata*) pelage color

77   recently experienced rapid change—likely due to an environmental shift (Galván et al.,

78   2019). Whether or not this will lead to environmental mismatch or rapid adaptive

79   evolution is yet to be seen. Mainly, this is due to a lack of data on the forces and

80   mechanisms that drive hair variation within primate populations. Thus, studying

81   population-level pelage color broadly relates to understanding wild primate adaptation (or

82   maladaptation).

83   Indriidae, a lemur family, is an ecologically diverse radiation of primates in

84   Madagascar that exhibits spectacular pelage diversity. Specifically, the coloration of

85   sifakas (*Propithecus* spp.) has been the subject of speculation for decades because of high

86   diversity in pelage color patterns with variable degrees of black coloration, both among

87   species and within populations (Mittermeier et al., 2010). Naturalists have documented

88   melanic (black) morphs since the mid-1900s in various sifaka populations—across

89   species that are not typically melanic. Early naturalists and recent empirical evidence

90   show dark morphs co-occur in colder forests (King et al., 2014; Pastorini et al., 2001;

91   Petter & Peyrieras, 1972; Tapanes et al., 2021). This pattern may implicate selection for

4

92   enhanced thermoregulation (Bogert's rule) because dark coat colors may aid in absorbing

93   heat from the sun's rays (Bogert, 1949; Delhey et al., 2019). However, some of these

94   populations have already gone locally extinct due to intense deforestation in Madagascar

95   (Tattersall, 1986).

96   Nevertheless, there is a unique opportunity to study hair color variation in a

97   population of diademed sifakas (*Propithecus diadema*) living in the unprotected forest of

98   Tsinjoarivo, Madagascar (19°41'S, 47°48'E). Here, sifakas exhibit an extraordinary

99   degree of color variation and facial patterning complexity (Figure 1) (Mittermeier et al.,

100   2010), and have been under study for 20+ years (Irwin, 2006; Irwin et al., 2019).

101   Throughout most of the species' range, diademed sifakas exhibit a tri-colored orange,

102   black, and white pelage. At Tsinjoarivo, unique coloration patterns include the classic tri-

103   colored morphotype, completely melanic individuals, partly melanic individuals (e.g.,

104   melanic from the dorsal torso upwards), and variations in between (Mittermeier et al.,

105   2010). Historically, geneticists considered placing Tsinjoarivo sifakas in a distinct taxon

106   (Rumpler et al., 2011) because their unique pelage coloration patterns are not typical of

107   the rest of the species' range (Groves, 2001). However, Tsinjoarivo sifakas are currently

108   subsumed into diademed sifakas and recognized as a non-distinct genetic population-

109   based on mitochondrial DNA (Mayor et al., 2004). Sifakas at Tsinjoarivo live in both

110   continuous and fragmented forest. Tsinjoarivo is also typified by a significant elevational

111   gradient–highest in the west (≈1600m) and lowest in the east (≈1350m). Previous climate

112   recordings from inside the forest indicate that more rain falls in the eastern-most block of

113   continuous forest on average (≈2600mm) in comparison with fragmented forest patches

114   in the west (≈2000mm) (Irwin, 2006). Thus, Tsinjoarivo sifakas represent an ideal case to

115   test what potential forces (e.g., climatic, demographic) underly primate coloration

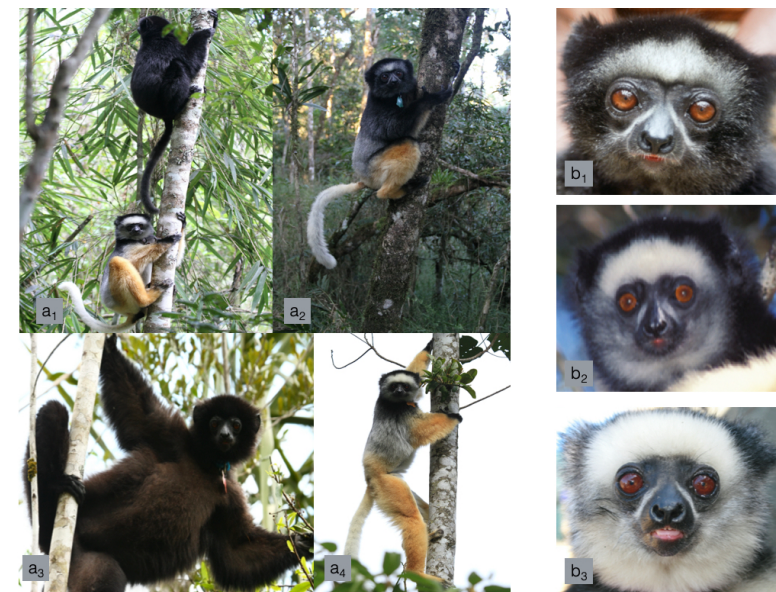116   variation within a wild primate population.

117

118
119   **Figure 1** Pelage color variation in diademed sifakas of Tsinjoarivo, Madagascar (a)
120   across the anterior body and (b) across the head
121
122   In this study, we first examined climatic variation across the Tsinjoarivo forest.

123   We were interested in determining whether variation in climatic regions, or lack thereof,

124   could provide insight into pelage variation. We hypothesized we would find significant

125   climate differences, based on previously recorded data at Tsinjoarivo that has not been

126   empirically tested (Irwin, 2006). We then analyzed photographs of wild sifakas living in

127   Tsinjoarivo over the past ≈20 years to test how climate and/or demography co-vary with

128   whole-body pelage pigmentation and pattern complexity. We predicted that pelage

129   morphs would be distributed randomly throughout the forest regardless of climate,

130   consistent with neutral evolution. Alternatively, we predicted pelage morphs may be

131   distributed in a non-random pattern. The latter would implicate either selection pressure

132   or restricted gene flow.

6

Methods

Climate Modelling

<u>Study site</u>

At Tsinjoarivo, we sampled fragmented (towards the west) and continuous forest (towards the east) through three base camps previously set up at Tsinjoarivo. From west to east, the first is Mahatsinjo camp (i.e., FRAG1-7, 19°40.94'S, 47°45.46'E) in the west, followed by Ankadivory camp (i.e., CONT4-5, 19°42.98'S, 47°49.29'E), and lastly by Vatateza camp (i.e., CONT1-3, 19°43.25'S, 47°51.41'E) (Figure 2). In general, the eastern-most continuous section of the forest has a higher canopy, fewer but larger trees, a higher basal area per hectare, and a higher quality forest compared to the western-most fragmented forest (Irwin, 2006; Irwin et al., 2019).
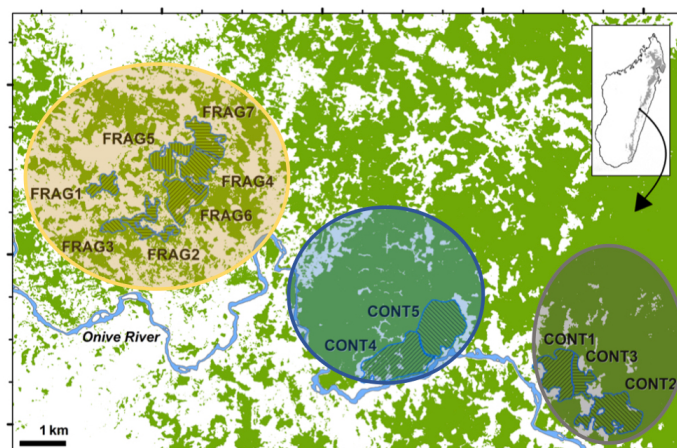

Figure 2 A detailed map of the spatial composition of all groups in Tsinjoarivo, Madagascar across three base camps. The yellow circle encompasses Mahatsinjo, the blue circle encompasses Ankadivory, and the grey circle encompasses Vatateza.

<u>Analyses</u>

We collected climate data using presence-only occurrence points for 13 sifaka groups across Tsinjoarivo, including seven groups from the fragmented forest and five

153   groups from the continuous forest, using WorldClim version 1 (Hijmans et al., 2005) at

154   30-sec (ca. 1km) spatial resolution. WorldClim is widely used in biogeography studies

155   (Fuchs et al., 2018) and has been used effectively in Madagascar despite the lower

156   number of weather stations (Pearson, 2015; Vieilledent et al., 2013). We confirmed three

157   extremely close (≈3km) weather stations to Tsinjoarivo and an additional six only ≈30-

158   40km in either direction (NE, SE, NW, SW). We clipped the data to the species range but

159   extended it out to the coast (using QGIS v3.10.1) because some diademed sifaka

160   populations currently live in forest remnants closer to the coast (i.e., Betampona).

161   Additionally, multiple Indriidae species likely occurred outside their current ranges as

162   little as 20-50 years ago due to rapid deforestation in Madagascar, especially the eastern

163   lowlands (Jungers et al., 1995).

164   We ran a correlation matrix of all 19 WorldClim bioclimatic variables (measuring

165   various aspects of rainfall and temperature) extracted across habitats in Tsinjoarivo (from

166   the 13 groups) and removed variables that exhibited correlation coefficients > 0.80. The

167   resulting dataset included six bioclimatic variables (SI: Table 1). We generated

168   Ecological Niche Models (ENMs) using Maxent v3.4.1 (Phillips, Dudik, & Schapire,

169   n.d.) with default settings. We estimated model performance using the area under the

170   receiver operating characteristic curve (AUC), and took models above 0.70 to indicate

171   good performance (Swets & Swets, 1988). ENMs can be used to assess the predicted

172   distribution of entire species (Elith & Leathwick, 2009; Elith et al., 2011). However,

173   recent studies indicate that ENMs on populations provide data on population

174   differentiation because subtle environmental differences can adequately reflect local

175   variation (Gonzalez et al., 2011; Soto-Centeno et al., 2013).

176   After generating ENMs, we used an identity test to assess the similarity between

177   models developed from fragmented vs. continuous habitat using the R package

178   'ENMTools' (Fuchs et al., 2018; Warren et al., 2010). We did not assess the differences

179   between each 'region' because we lacked statistical power to divide an already small

180   sample. The test took locality data from continuous and fragmented habitat groups and

181   randomly assigned localities to "pseudo" habitat pairs (also known as "pseudo" species

182   pairs in macro-scale studies). The test then took known locality points and randomized

183   their identities to produce a new dataset composed of the same number of localities as the

184   original input data. In total, we generated 99 pseudo habitat pairs and then compared

185   pseudo-pairs to the real habitat data. We supplemented this with estimates of predicted

186   similarity between both habitats using the niche overlap function in ENMtools based

187   on *Schoener's D* (Schoener, 1968) and *Hellinger's I* (both range from 0 to 1) (Warren et

188   al., 2010). A value of one indicates complete niche overlap, and zero indicates no niche

189   overlap. Similarly, we generated 99 pseudo habitat pairs for *D* and *I* and compared

190   observed values to the random distributions. If the observed values fell below the

191   randomized values, no significant niche or climate overlap existed.

192   To further assess the Maxent models' success, we performed a binomial omission

193   test under a minimum training presence, at an alpha of 0.025. We followed a four-fold

194   cross-validation approach. Due to our dataset's small size, we withheld approximately

195   40% of occurrences in each habitat type as test data (e.g., 2 of 5 of continuous

196   occurrences, 3 of 7 of fragmented). We randomly shuffled occurrences into test and train

197   splits for each fold. Lastly, in our pelage analysis below, we used the two climate

198   variables with the highest permutation of importance (SI: Table 2).

9

199

200 *Pelage variation*

201 <u>Sampling and Photo Collection</u>

202 In this study, we examined hair color variation across Tsinjoarivo sifakas. We

203 habituated groups before capturing and then captured animals at close range using Pneu-

204 dart 9mm disposable non-barbed darts. A trained professional performed the

205 immobilization with tiletamine/zolazepam (Telazol). Medical examinations followed a

206 standard protocol established by the Prosimian Biomedical Survey Project (PBSP) Team

207 and used on 750+ lemurs, over 16 sites, and 35 species since 2000 (Dutton et al., 2003;

208 Irwin et al., 2010).

209 We took ≈20-30 digital photographs and/or slides of each sifaka during captures

210 using an existing standard protocol (Irwin et al., 2010). Our sampling thus spanned ≈20

211 years' worth of photos across different cameras and lighting conditions (N =87; SI: Table

212 3). We did not remove any phenotypic outliers because that would require removing the

213 most exciting variants (i.e., all melanic) in the sample and thus negating the purpose of

214 the study.

215

216 <u>Ethical Note</u>

217 We performed the research according to Madagascar's ethical and legal

218 requirements and the Code of Best Practices for Field Primatology. The study was

219 ethically reviewed and approved by the IACUC (Institutional Animal Care and Use

220 Committee) of Northern Illinois University (LA12-0011), University of Queensland,

221 McGill University, and Stony Brook University. A team captured sifakas for ongoing

222   parallel research, including population monitoring, sample collection, and conservation

223   efforts—and not to study their hair variation. Therefore, our photographic sampling was

224   opportunistic.

225

226   <u>Semi-Quantitative Scoring</u>

227   We developed a systematic method of scoring pelage variation semi-

228   quantitatively (Figure 3) based on similar pelage scoring systems from previous studies

229   in other primates (Caro et al., 2021; Rakotonirina et al., 2017; Santana et al., 2012;

230   2013). Two individuals scored sifaka photographs, and we verified intra- and

231   interscorer reliability above 95%. Photos were blind coded. One scorer was unaware of

232   hypotheses behind the study and locality of individual sifakas. The second scorer was

233   unaware of the locality of the sifaka photos (but aware of hypotheses). We scored 18

234   Tsinjoarivo sifaka body regions on coloration, complexity, and contrast across a large

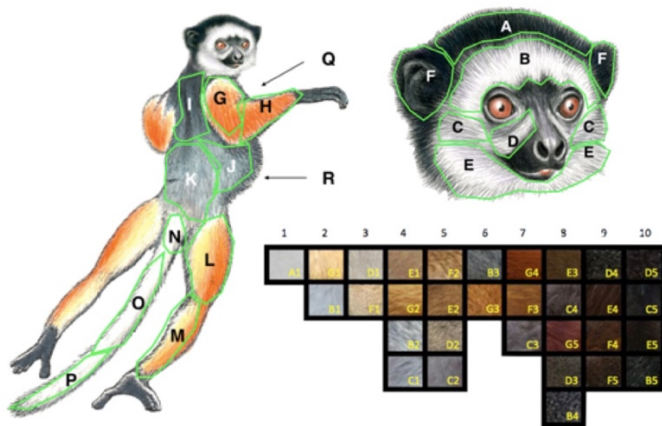235   sample (N = 87; SI: Table 4).

236

237   **Figure 3** Scoring schematic use to characterize pelage variation in this study. The scoring
238   chart was adapted from a previous study (Caro et al., 2017). Sifaka illustrations modified
239   with permission, copyright 2013 Stephen D. Nash.

240

241   For every sifaka, we assigned each region a score (1-10) and a shade (31

242   possible; A1-G5) from 10-15 photos. For example, a completely orange lower forelimb

243   (region H) scored a "6" in coloration and "G3" as the shade (Figure 3). We used

244   numerical scores to calculate mean pigmentation scores, and letter scores (e.g., A1) to

245   calculate complexity and contrast scores. We defined pattern complexity as the total

246   number of shades (31 possible) across each central body region (e.g., head), and

247   contrast as the difference in the most extreme shades of each significant body region (on

248   a scale of 1-10). We estimated body coloration (brightness/darkness) as the mean

249   numerical score (1-10) of all shades per area, per individual (SI: Table 4). We measured

250   complexity and contrast using subsumed scores from the head, anterior body, and

251   ventral-torso scores. We measured pigmentation from subsumed variables from the

252   head, dorsal-torso, hindlimb, forelimb, ventral-torso, and tail regions. We measured

253   countershading as the ratio between the ventral and dorsal pigmentation scores. For any

254   individuals that were captured twice (across distinct years), we computed their mean

255   pigmentation score (1-10) to assess brightness/overall color (i.e., darkness). Color

256   scores did not vary over time. In body regions where more than one color/shade was

257   evident in the coat/body region, we assigned scores based on the predominant color

258   (Caro et al., 2017).

259   We note that despite criticisms that the human visual system distorts animal

260   colors (Stevens et al., 2009), the human visual system may be good at detecting animal

261   color variation in the general visible spectrum. Specifically, recent work shows that

262   color extracted from images (using sets of ≈12, as we did) can be reliable—this may be

263   particularly true for estimates, such as these, of dark or light coloration (Higham, 2021;

264   Laitly et al., 2021).

265

266   <u>Analyses</u>

267   We conducted two principal components analyses (PCA) on numerical pelage

268   variables using R's prcomp function (R Core Team, 2018). We removed pelage

269   variables with highly correlated vectors (i.e., overlapped in the biplot) to reduce the

270   dimensionality of the data and meet parametric testing assumptions. The first PCA

271   included body pigmentation (brightness/darkness) scores, and the second PCA included

272   pattern complexity (including contrast and countershading). Henceforth, we will refer to

273   the first as the 'brightness PCA' and the latter as the 'pattern PCA.' We used transformed

274   PC scores (eigenvalues > 1) as dependent variables (Kaiser, 1960) in general linear

275   regression models. We positivized all PC values by adding a constant (the absolute

276   value of the lowest PC score) to each value.

277   We ran general linear models that included several predictor variables. To assess

278   impacts from climate/ecology, we used the two climate variables that contribute to

279   climate differences across Tsinjoarivo (along with age-class and sex-class) as our

280   independent variables. We used the dredge function in the MuMIn package (Barton,

281   2019) for model selection based on Akaike's Information Criterion with modification

282   for small sample size (AICc). AICc scores provided us with the likelihood of a model

283   given a dataset while minimizing model complexity. Models within two AICc values of

284   the "best model" were deemed equally good (Burnham & Anderson, 2003; Wheeler et

285   al., 2011). We calculated each model's weight as a supplement to determining the best

286   fit model, which was particularly useful when multiple models had similar AICc scores.

287   Then, we assessed each predictor variable's importance in our models based on their

288   sum of AICc weights. We used G*Power (Faul et al., 2009) to determine our linear

289   models' statistical power. Given our sample size, the number of predictor variables, and

290   the use of a two-tailed general linear regression, we estimated we could detect a small

291   effect size (.29) with 85% power.

292

293   *Data Availability Statement*

294   The datasets generated and analyzed for the current study are available from the

295   corresponding author on reasonable request.

296

297   **Results**

298   *Climate Modelling*

299   Models had a mean AUC value above 0.98—which indicated high performance.

300   Our models showed a significant climate dissimilarity between fragmented forest groups

301   in the west and the east's continuous forest groups (Figure 4). This gradient is potentially

302   formed because continuous forest sits at a lower elevation than fragmented forest. Our

303   observed values of *Shoener's D* and *Hellinger's I* were outside the range of the random

304   distribution of values (SI: Figure 1) and statistically distinct (identity test, $p = 0.01$) (SI:

305   Table 5). Additionally, the binomial test of omission was significant across continuous

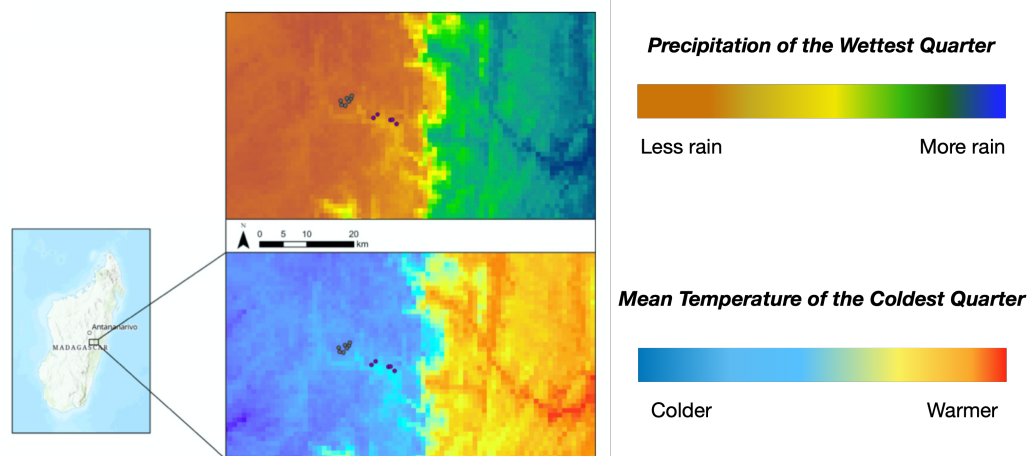306   and fragmented forests across all four-folds ($p < 0.0001$) (SI: Table 6).

307

14

Figure 4 A west-east gradient that is formed in Tsinjoarivo, based on 'Precipitation of the Wettest Quarter' and 'Mean Temperature of the Coldest Quarter'

Several variables distinguished fragmented and continuous forest habitat models. The highest permutation importance to the fragmented forest habitat model included precipitation of the wettest quarter (bio16) at ≈38%, but for the continuous forest, it was mean temperature of the coldest quarter (bio11) at 56%. Temperature annual range (bio07) was the second-highest contributor to both models' permutations at 33% (SI: Table 4). These variables indicate a west-east gradient in precipitation and temperature across Tsinjoarivo (Figure 4).

Pelage variation

Regarding the 'brightness PCA,' we found that the first PC (eigenvalue > 1) explained ≈62% of the variation in the dataset (Figure 5). Loadings on PC1 included forelimb coloration (.29), dorsal torso coloration (.25), ventral torso coloration (.24), and tail coloration (.20). We found a significant association between PC1 and both climate variables (precipitation of the wettest quarter (BIO16) and temperature of the coldest quarter (BIO11)) (Table 1). From this point forward, we refer to these climate

15

328 variables as 'precipitation' and 'temperature,' respectively. We note that PC1 increases

329 as temperature increases (i.e., pelage gets lighter) (Table 1, Figure 5). Specifically, this

330 'brightness PCA' illustrates that darker individuals in our sample most often lived in

331 colder forest patches that exhibited less precipitation (Figure 5). In the best-fit models

332 for PC1, according to AICc scores, the strongest predictors were climate variables and

333 age class (SI: Table 7). However, our general linear model detected no significant

334 differences across sex-class or age-class (Table 1). Additionally, both climate variables

335 contributed ≈50% and ≈75% more to the model than either age-class or sex-class,

336 respectively (SI: Table 8).

337
338 **Table 1** General linear model (GLM) predicting the PC1 values of the pigmentation PCA
339 while including all independent variables.

	Estimate	Std. Error	T-value	P-value
PC1				
Intercept	33.035	5.959	5.544	**< 0.0001**
BIO16	-0.330	0.068	-4.808	**< 0.0001**
BIO11	18.022	3.890	4.621	**< 0.0001**
AgeClass	-0.311	0.203	-1.536	0.128
Sex	-0.079	0.300	-0.261	0.795

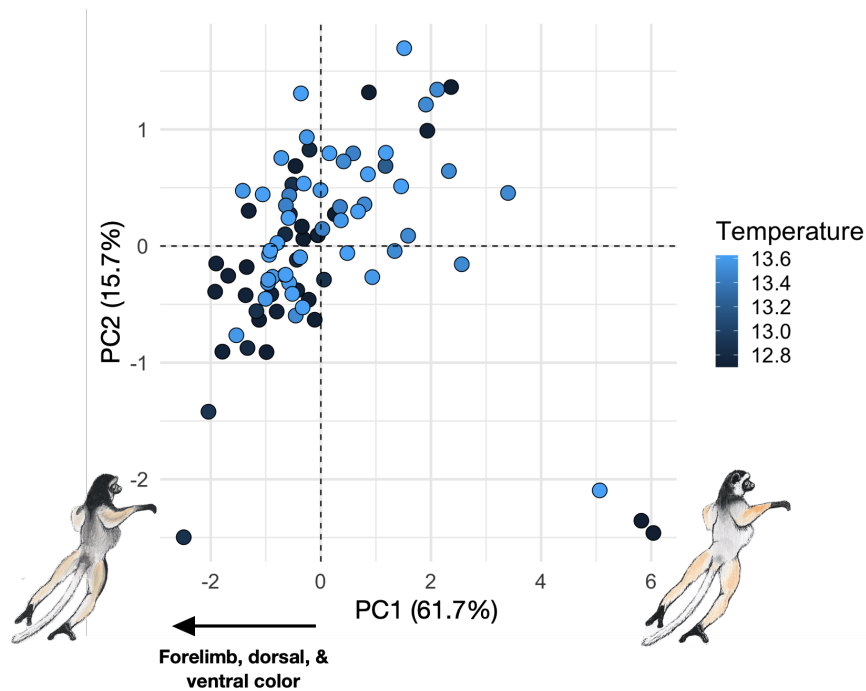340 Bold values indicate significance below p = 0.05

341

Figure 5 Plot of PCA scores representing overall pelage coloration of Tsinjoarivo sifakas across the climate gradient (shown with temperature). Brightness increases with increasing PCA values (and darker sifakas are represented by lower PC values).

For the 'pattern PCA' (to assess complexity), the first two PCs (eigenvalues > 1) explained ≈60% of the variation in the dataset (Figure 6). Highest loadings on PC1 included head color complexity (.39), head color contrast (.37), ventral torso color contrast (.24), ventral torso color complexity (.0), and countershading (.0). Specifically, we detected a statistically significant effect of temperature and precipitation on PC1 (Table 2), with temperature being negatively related to PC1 (Table 2). This indicates PC1 would be expected to increase (i.e., complexity increase) as temperatures increase, as indicated by the PCA (Figure 6).
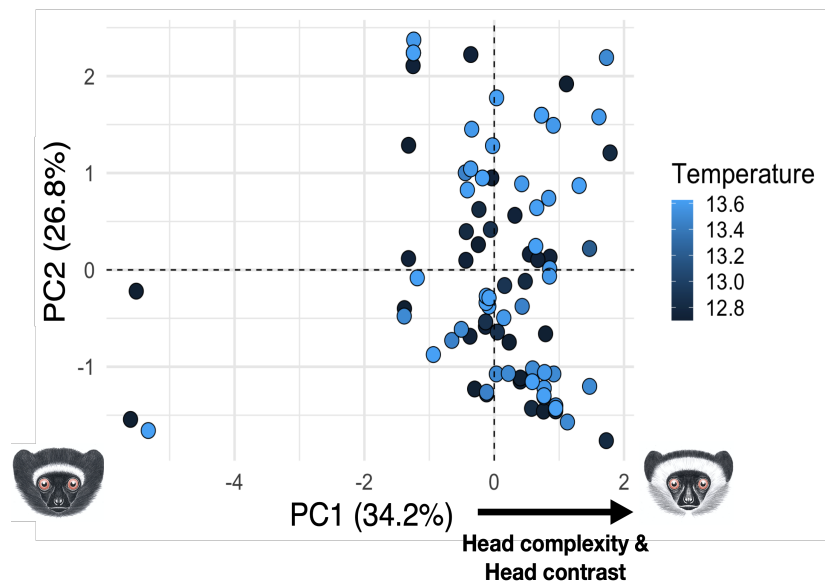
Figure 6 Plot of PCA scores representing the pelage complexity of Tsinjoarivo sifakas across the climate gradient. Less complex pelage is represented by lower PC values.

Furthermore, we did not detect a significant association between PC1 and age or sex class. According to AICc scores, only the two climate variables contributed to the best fit model for PC1 (SI: Table 9). Climate variables contributed ≈30% and 40% more to PC1 than either sex-class or age-class, respectively (SI: Table 10). Loadings on PC2 include countershading (.45), ventral torso color complexity (.45), ventral torso color contrast (.08), head color contrast (.03), and head color complexity (0). We did not detect statistically significant effect of any predictor on PC2. Climate variables alone accounted for the model with the second-best fit for patterning PC2 (SI: Table 10). No variables contributed to the model in the best-fit model for PC2 (SI: Table 11). Climate variables contributed ≈10% and ≈20% more than both sex-class and age-class, respectively (SI: Table 12).

18

375 **Table 2** General linear model (GLM) summary predicting PC1 and PC2 of the color
376 patterning PCA using all independent variables.

	Estimate	Std. Error	T-value	P-value
PC1				
Intercept	0.911	5.566	0.164	0.870
BIO16	0.128	0.064	2.000	**0.049**
BIO11	-7.685	3.643	-2.109	**0.038**
AgeClass	0.116	0.189	0.611	0.543
Sex	0.046	0.280	0.148	0.882
PC2				
Intercept	9.091	4.923	1.847	0.068
BIO16	-0.105	0.057	-1.860	0.066
BIO11	5.883	3.222	1.826	0.072
AgeClass	-0.214	0.167	-1.276	0.206
Sex	-0.269	0.248	-1.087	0.280

377 Bold values indicate significance below p = 0.05

378

379 **Discussion**

380   This study documents that pigmentation varies with climate across a small

381 geographical scale in a wild lemur population. At Tsinjoarivo, a climate gradient is

382 formed—likely due to the forest being a "high altitude island" and cross-cutting two

383 Köppen climate zones. This unique combination creates a colder and less rainy climate at

384 the highest altitude, which is also the most fragmented habitat. Respectively, both whole

385 body pelage color (Table 1) and facial complexity (Table 2) were associated with climate

19

386   variables. Specifically, darker individuals with less complex faces also occur most often

387   in this colder, less rainy, more fragmented western forest (Figure 5, Figure 6). However,

388   it is not easy to arrive at any firm conclusions for the mechanism behind the observed

389   pattern without genetic evidence. There are, though, three potential hypotheses that may

390   explain the pattern: (1) isolation by distance, (2) an environmental gradient, or (3) local

391   adaptation. We flesh out intricacies of all three below and set up predictions that would

392   support each hypothesis based on work in other taxa.

393   The most parsimonious explanation for the pattern in our data is a scenario of

394   isolation by distance (Kimura et al., 1993; Slatkin et al. 1993). First, relatedness may be a

395   confounding factor across our analyses because individuals living in closer proximity are

396   also more likely to be related to each other. This may explain why individuals of similar

397   phenotype cluster together in geographic space (Figure 5). Although we do not have

398   enough data to estimate heritability, from anecdotal observations, we know that offspring

399   can exhibit distinct coloration from their mothers (i.e., fully melanic offspring born to tri-

400   colored mothers). Relatedness aside, forest fragmentation may impede gene flow out of

401   the fragmented forest and create substructure within the population. Thus, individuals in

402   the fragmented forest could also be darker due to inbreeding and/or low genetic diversity.

403   Rare (often melanic) pigmentation phenotypes can arise in other taxa due to increased

404   inbreeding (Larison et al., 2021) or population bottlenecks (Sagar et al., 2021). Although

405   previous work indicates identical mitochondrial haplotypes in groups sampled across

406   Tsinjoarivo, mitochondrial DNA may not always accurately estimate relatedness between

407   individuals or populations (Guschanski et al., 2013; Mayor et al., 2004; Meyer et al.,

408   2016). However, testing the hypothesis of isolation by distance would require genomic

409 evidence we do not yet have. Results supporting this hypothesis may show evidence of

410 restricted gene flow between distinct groups and/or population structure across non-

411 coding and non-outlier loci. An argument against this hypothesis is that there is evidence

412 that sifakas are resilient to fragmentation, as they do not often show decreased gene flow

413 or population structure across fragmented habitats (Quéméré et al., 2010; Salmona et al.,

414 2015; Sgarlata et al., 2016). Sifakas also exhibit high levels of standing genetic

415 variation—the highest observed among primates—despite experiencing a bottleneck

416 ≈100,000 years ago (Guevara et al., 2021). High levels of genome-wide heterozygosity,

417 such as those seen in sifakas, can mean that there is sufficient genetic variation

418 immediately available for selection to act upon when environmental conditions change—

419 thereby increasing the likelihood of rapid adaptive evolution (Barrett & Schluter, 2008).

420 Thus, this phenotypic pattern may be indicative of selection acting across an

421 environmental gradient. There are two main climate gradients in Madagascar: a North-

422 South gradient in temperature and a West-East gradient in precipitation. Additionally,

423 temperatures decrease as altitudes increase towards the central plateau (Irwin, 2006;

424 Kamilar & Muldoon, 2010). Temperature shows the most significant effect in our models

425 (Table 1, Table 2). Specifically, we found that darker torso and limb color was associated

426 with colder forests with less precipitation (Figure 5). This result supports the thermal

427 melanism hypothesis (i.e., Bogert's rule) that argues darker fur aids with

428 thermoregulation in colder forests because dark colors may derive more heat from sun

429 rays (Bogert, 1949). Although Bogert's rule is most commonly used to explain coloration

430 patterns in ectotherms (Bishop et al., 2016; Xing et al., 2016), recent findings extend the

431 rule to birds and mammals (Delhey, 2018; Tapanes et al., 2021). Specifically, Bogert's

21

432   rule explains patterns of pelage color variation at a genus-wide level across *Propithecus*,

433   which may implicate thermoregulation as a central selective force in the genus (Tapanes

434   et al., 2021). Tsinjoarivo sifakas, unsurprisingly then, live at the highest altitude and

435   southernmost end of their range. To the North of the diademed sifaka range is the

436   brighter/whiter silky sifaka (*P. candidus*) and to the South is the darker and more melanic

437   Milne-Edwards's sifaka (*P. edwardsi*) (Mittermeier et al., 2010). Yet evidence for this

438   hypothesis would need to demonstrate that environmental factors, not geographic

439   distance, explain a significant proportion of sifaka genetic variation (McCairns &

440   Bernatchez, 2008).

441   Another alternative is that, high levels of standing genetic variation (as in sifakas)

442   may increase the efficacy of selection, driving local adaptation within specific

443   populations driven by other selective forces (i.e., not thermoregulation) (Woolridge et al.,

444   2021). A pattern of uniquely locally adapted pelage across Tsinjoarivo is unlikely but

445   would also explain the cluster of darker individuals (as well as less pelage complexity) in

446   colder more fragmented forest. To explain the latter, warm wet regions are assumed to be

447   associated with denser forest habitats—thus, more complex faces in the eastern denser

448   forest may aid with conspecific signal visibility (and potentially inbreeding avoidance

449   (Allen et al., 2014)). However, primate faces exhibit high degrees of phylogenetic signal,

450   thus genetic drift could be driving facial pattern complexity in our data (Bell et al., 2021;

451   Rakotonirina et al., 2017). Other pelage phenotypes (such as degree of redness) may be

452   more salient for signaling, especially given this population of sifakas is polymorphic

453   trichromatic (Jacobs et al., 2017; Tapanes et al., 2021). Nevertheless, under the

454   assumption of high gene flow high across the Tsinjoarivo landscape (as in other sifaka

455   populations), adaptation would have to be strong enough to overcome migration (i.e.,

456   selection-migration dynamics) (Haldane, 1930). The mutations underlying phenotypic

457   divergence in this scenario would thus have to be few in number, of large effect, and/or in

458   close proximity (Yeaman & Whitlock, 2011). Thus, genomic evidence for local

459   adaptation within this sifaka population would implicate either one outlier loci of large

460   effect (i.e., *MC1R*, *KITLG*) or many outlier loci of small effect which are gnomically

461   clustered (Pfeifer et al., 2018). All three potential hypothesis should be explored fully

462   with whole exome and/or whole genome data.

463   However, regardless of the mechanism maintaining phenotypic divergence in this

464   sifaka population, these phenotypic patterns may carry significant implications for

465   conservation. If isolation by distance produces the phenotypic pattern detected here, it

466   would mean that there is limited gene flow between sifakas in fragmented forest and

467   those in continuous forest. Generally, fragmented forest in Tsinjoarivo is low quality

468   habitat and sifakas living there exhibit physiological signs of stress (i.e., low body mass,

469   low white blood cell counts) (Irwin et al., 2008a; 2008b; 2010; 2019). Given predation

470   rates by fosa are higher in fragmented forest (Irwin et al., 2009), isolation may signal the

471   eventual demise of groups living in the fragments. Alternatively, if local adaptation or a

472   larger environmental gradient is responsible for the current pattern, it may foretell future

473   maladaptation and potentially local extinction for the population—because loss of habitat

474   where a population has been uniquely adapted to thrive may drive environmental

475   mismatch. Such a mismatch can have consequences, such as increased predation on

476   maladapted phenotypes (e.g., a mismatch between pelage and background color). Either

477   scenario thus poses a significant risk to the already Critically Endangered diademed

478   sifaka and the unprotected forest of Tsinjoarivo (which harbors high levels of

479   biodiversity) (Goodman et al., 2000; Irwin, 2020). It's likely that across other

480   populations, hair variation may also serve as a signal of adaptation, environmental

481   mismatch, or restricted gene flow. However, such data is missing in the primatological

482   literature, thus, it remains unknown if the patterns detected across Tsinjoarivo sifakas are

483   exceptional or typical.

484

485   **Conflicts of Interest:** The authors declare that they have no conflicts of interest.

486

501   Zamora for feedback on earlier drafts of this manuscript, as well as anonymous reviewers

502   and an editor that provided useful feedback for us to effectively revise a previous version

503   of this manuscript.

504

505

506

507

508

509

510

511

512

513

514

515

516

517

518

519

520

521

522

523

524 **References**

525 Allen, W. L., Stevens, M., & Higham, J. P. (2014). Character displacement of

526   Cercopithecini primate visual signals. *Nature Communications*, *5*, 1–10.

527   https://doi.org/10.1038/ncomms5266

528 Barrett, R. D. H., & Schluter, D. (2008). Adaptation from standing genetic variation.

529   *Trends in Ecology and Evolution*, *23*(1), 38–44.

530   https://doi.org/10.1016/j.tree.2007.09.008

531 Barton, K. (2009). MuMln: *Multi-Model inference. R package version 1.43.15*. http://r-

532   forge/r-project.org/projects/mumin

533 Bell, R. B., Bradley, B. J., & Kamilar, J. M. (2021). The Evolutionary Ecology of

534   Primate Hair Coloration : A Phylogenetic Approach. *Journal of Mammalian*

535   *Evolution*, 28, 911-927.

536 Bishop, T. R., Robertson, M. P., Gibb, H., van Rensburg, B. J., Braschler, B., Chown, S.

537   L., … Parr, C. L. (2016). Ant assemblages have darker and larger members in cold

538   environments. *Global Ecology and Biogeography*, *25*(12), 1489–1499.

539   https://doi.org/10.1111/geb.12516

540 Bogert, C. M. (1949). Thermoregulation in reptiles, a factor in evolution. *Evolution*, *3*,

541   195–211. https://doi.org/10.1111/j.1558-5646.1949.tb00021.x

542 Bradley, B. J., & Mundy, N. I. (2008). The primate palette: The evolution of primate

543   coloration. *Evolutionary Anthropology*, *17*(2), 97–111.

544   https://doi.org/10.1002/evan.20164

545 Burnham, K. P., & Anderson, D. (2003). *Model selection and multi-model inference: A*

546   *Practical Information-Theoretical Approach (2nd ed.)*. New York: Springer.

547 Caro, T., Brocelsby, K., Ferrari, A., Koneru, M., Ono, K., Touche, E., & Stankowich.

548   (2021). The evolution of primate coloration revisited. *Behavioral Ecology*, *32*(4),

549   555–567.

550 Caro, T., & Mallarino, R. (2020). Coloration in Mammals. *Trends in Ecology and*

551   *Evolution*, *35*(4), 357–366. https://doi.org/10.1016/j.tree.2019.12.008

552 Caro, T., Stoddard, M. C., & Stuart-Fox, D. (2017). Animal coloration: production,

553   perception, function and application. *Philosophical Transactions of the Royal*

554   *Society B: Biological Sciences*. https://doi.org/10.1098/rstb.2017.0047

555 Caro, T., Walker, H., Santana, S. E., & Stankowich, T. (2017). The evolution of anterior

556   coloration in carnivorans. *Behavioral Ecology and Sociobiology*, *71*(12).

557   https://doi.org/10.1007/s00265-017-2402-5

558 Cuthill, I. C., Allen, W. L., Arbuckle, K., Caspers, B., Chaplin, G., Hauber, M. E., …

559   Caro, T. (2017). The biology of color. *Science*, *357*(6350).

560   https://doi.org/10.1126/science.aan0221

561 Delhey, K. (2018). Darker where cold and wet: Australian birds follow their own version

562   of Gloger's rule. *Ecography*, *41*(4), 673–683. https://doi.org/10.1111/ecog.03040

563 Delhey, K., Dale, J., Valcu, M., & Kempenaers, B. (2019). Reconciling ecogeographical

564   rules: rainfall and temperature predict global colour variation in the largest bird

565   radiation. *Ecology Letters*, *22*(4), 726–736. https://doi.org/10.1111/ele.13233

566 Dutton, A., Christopher, J., & Randall, E. (2003). Biomedical evaluation of free-ranging

567   ring-tailed lemurs (*Lemur catta*) in Tsimanampetsotsa Strict Nature Reserve,

568   Madagascar. *Journal of Zoo and Wildlife Medicine*, *34*(1), 16–24.

569   https://doi.org/10.1638/1042-7260(2003)34[0016:beofrl]2.0.co;2

27

570   Elith, J., & Leathwick, J. R. (2009). Species distribution models: Ecological explanation

571   and prediction across space and time. *Annual Review of Ecology, Evolution, and*

572   *Systematics*, *40*(1), 677–697.

573   https://doi.org/10.1146/annurev.ecolsys.110308.120159

574   Elith, J., Phillips, S. J., Hastie, T., Dudík, M., Chee, Y. E., & Yates, C. J. (2011). A

575   statistical explanation of MaxEnt for ecologists. *Diversity and Distributions*, *17*(1),

576   43–57. https://doi.org/10.1111/j.1472-4642.2010.00725.x

577   Faul, F., Erdfelder, E., Buchner, A., & Lang, A. G. (2009). Statistical power analyses

578   using G*Power 3.1: Tests for correlation and regression analyses. *Behavior*

579   *Research Methods*, *41*(4), 1149–1160. https://doi.org/10.3758/BRM.41.4.1149

580   Fuchs, A. J., Gilbert, C. C., & Kamilar, J. M. (2018). Ecological niche modeling of the

581   genus *Papio*. *American Journal of Physical Anthropology*, *166*(4), 812–823.

582   https://doi.org/10.1002/ajpa.23470

583   Galván, I., Jorge, A., Sánchez-Murillo, F., & Gutiérrez-Espeleta, G. (2019). A recent shift

584   in the pigmentation phenotype of a wild Neotropical primate. *Mammalian Biology*,

585   *94*, 66–68. https://doi.org/10.1016/j.mambio.2018.10.007

586   Gonzalez, S. C., Soto-Centeno, J. A., & Reed, D. L. (2011). Population distribution

587   models: Species distributions are better modeled using biologically relevant data

588   partitions. *BMC Ecology*, *11*, 20. https://doi.org/10.1186/1472-6785-11-20

589   Goodman, Steven M., Rakotondravony, D., Raherilalao, M. J., Rakotomalala, D.,

590   Raselimanana, A. P., Soarimalala, A., … Rafanomezantsoa, J. (2000). Inventaire

591   biologique de la forêt de Tsinjoarivo, Ambatolampy. *Akon'ny Ala*, *27*, 18–27.

592   Groves, C. (2001). *Primate taxonomy*. Smithsonian Books.

593   Guevara, E. E., Webster, T. H., Lawler, R. R., Bradley, B. J., Greene, L. K.,

594   Ranaivonasy, J., … Rogers, J. (2021). Comparative genomic analysis of sifakas

595   (*Propithecus*) reveals selection for folivory and high heterozygosity despite

596   endangered status. *Science Advances*, *7*(17), 1–13.

597   https://doi.org/10.1126/sciadv.abd2274

598   Guschanski, K., Krause, J., Sawyer, S., Valente, L. M., Bailey, S., Finstermeier, K., …

599   Savolainen, V. (2013). Next-generation museomics disentangles one of the largest

600   primate radiations. *Systematic Biology*, *62*(4), 539–554.

601   https://doi.org/10.1093/sysbio/syt018

602   Haldane, J. (1930). *Enzymes long*. London/New York: Longmans, Green and Co.

603   Higham, J. P. (2021). Studying the color of monkeys: A comment on Caro et al.

604   *Behavioral Ecology*, *32*(4), 570-571. https://doi.org/10.1093/beheco/arab041

605   Hijmans, R. J., Cameron, S. E., Parra, J. L., Jones, P. G., & Jarvis, A. (2005). Very high

606   resolution interpolated climate surfaces for global land areas. *International Journal*

607   *of Climatology*, *25*(15), 1965–1978. https://doi.org/10.1002/joc.1276

608   Irwin, M.T. (2006). *Ecological impacts of forest fragmentation on diademed sifakas*

609   *(Propithecus diadema) at Tsinjoarivo, eastern Madagascar: Implications for*

610   *conservation in fragmented landscapes* (Publication No. 3239003) [Doctotal

611   Dissertation, Stony Brook University], ProQuest Dissertations and Theses.

612   Irwin, Mitchell T. (2008a). Diademed sifaka (*Propithecus diadema*) ranging and habitat

613   use in continuous and fragmented forest: Higher density but lower viability in

614   fragments? *Biotropica*, *40*(2), 231–240. https://doi.org/10.1111/j.1744-

615   7429.2007.00368.x

616   Irwin, Mitchell T. (2008b). Feeding ecology of *Propithecus diadema* in forest fragments

617   and continuous forest. *International Journal of Primatology*, *29*(1), 95–115.

618   https://doi.org/10.1007/s10764-007-9222-9

619   Irwin, Mitchell T. (2020). *Propithecus diadema*. Retrieved December 12, 2021, from The

620   IUCN Red List of Threatened Species website:

621   https://dx.doi.org/10.2305/IUCN.UK.2020-2.RLTS.T18358A115572884.en

622   Irwin, Mitchell T., Junge, R. E., Raharison, J. L., & Samonds, K. E. (2010). Variation in

623   physiological health of diademed sifakas across intact and fragmented forest at

624   Tsinjoarivo, eastern Madagascar. *American Journal of Primatology*, *72*(11), 1013–

625   1025. https://doi.org/10.1002/ajp.20847

626   Irwin, Mitchell T., Raharison, J. L., & Wright, P. C. (2009). Spatial and temporal

627   variability in predation on rainforest primates: Do forest fragmentation and

628   predation act synergistically? *Animal Conservation*, *12*(3), 220–230.

629   https://doi.org/10.1111/j.1469-1795.2009.00243.x

630   Irwin, Mitchell T., Samonds, K. E., Raharison, J. L., Junge, R. E., Mahefarisoa, K. L.,

631   Rasambainarivo, F., … Glander, K. E. (2019). Morphometric signals of population

632   decline in diademed sifakas occupying degraded rainforest habitat in Madagascar.

633   *Scientific Reports*, *9*(1), 1–14. https://doi.org/10.1038/s41598-019-45426-2

634   Jablonski, N. G., & Chaplin, G. (2017). The colours of humanity: The evolution of

635   pigmentation in the human lineage. *Philosophical Transactions of the Royal Society*

636   *B: Biological Sciences*, *372*(1724). https://doi.org/10.1098/rstb.2016.0349

637   Jacobs, R. L., MacFie, T. S., Spriggs, A. N., Baden, A. L., Morelli, T. L., Irwin, M. T., …

638   Bradley, B. J. (2017). Novel opsin gene variation in largebodied, diurnal lemurs.

639   *Biology Letters*, *13*(3), 1–6. https://doi.org/10.1098/rsbl.2017.0050

640   Jones, M. R., Mills, L. S., Alves, P. C., Callahan, C. M., Alves, J. M., Lafferty, D. J. R.,

641   … Jensen, J. D. (2018). Adaptive introgression underlies polymorphic seasonal

642   camouflage in snowshoe hares. *Science*, *1358*, 1355–1358.

643   https://doi.org/10.1126/science.aar5273

644   Jungers, W. L., Godfrey, L. R., & Simons, E. L. (1995). Subfossil *Indri indri* from the

645   Ankarana Massif of northern Madagascar. *American Journal of Physical*

646   *Anthropology, 97*(4), 357–366.

647   Kaiser, H. F. (1960). The application of electronic computers to factor analysis.

648   *Educational and Psychological Measurement*, *20*(1), 141–151.

649   https://doi.org/10.1177/001316446002000116

650   Kamilar, J. M., & Muldoon, K. M. (2010). The climatic niche diversity of Malagasy

651   primates: A phylogenetic perspective. *PLoS ONE*, *5*(6).

652   https://doi.org/10.1371/journal.pone.0011073

653   Kimura, M., & Weiss, G. H. (1964). The stepping stone model of population structure

654   and the decrease of genetic correlation with distance. *Genetics*, *49*(4), 561–576.

655   https://doi.org/10.1093/genetics/49.4.561

656   King, T., Rakotonirina, L. H. F., Rakotoarisoa, A. H., Razafindramanana, J., &

657   Ratsimbazafy, J. (2014). Distributional limits and melanism in the south-west of the

658   range of the crowned sifaka (*Propithecus coronatus*), Madagascar. *Primate*

659   *Conservation*, *28*(1), 55–64. https://doi.org/10.1896/052.028.0109

660   Laitly, A., Callaghan, C. T., Delhey, K., & Cornwell, W. K. (2021). Is color data from

661   citizen science photographs reliable for biodiversity research? *Ecology and*

662   *Evolution*, *11*(9), 4071–4083. https://doi.org/10.1002/ece3.7307

663   Larison, B., Kaelin, C. B., Harrigan, R., Henegar, C., Rubenstein, D. I., Kamath, P., …

664   Barsh, G. S. (2021). Population structure, inbreeding and stripe pattern

665   abnormalities in plains zebras. *Molecular Ecology*, *30*(2), 379–390.

666   https://doi.org/10.1111/mec.15728

667   Mayor, M. I., Wright, P. C., Sommer, J. A., Louis Jr., E. E., Houck, M. L., Zaonarivelo,

668   J. R., … Engel, S. R. (2004). Specific status of *Propithecus* spp. *International*

669   *Journal of Primatology*, *25*(4), 875–900.

670   https://doi.org/10.1023/B:IJOP.0000029127.31190.e9

671   McCairns, R. J. S., & Bernatchez, L. (2008). Landscape genetic analyses reveal cryptic

672   population structure and putative selection gradients in a large-scale estuarine

673   environment. *Molecular Ecology*, *17*(17), 3901–3916.

674   https://doi.org/10.1111/j.1365-294X.2008.03884.x

675   Meyer, M., Arsuaga, J. L., De Filippo, C., Nagel, S., Aximu-Petri, A., Nickel, B., …

676   Pääbo, S. (2016). Nuclear DNA sequences from the Middle Pleistocene Sima de los

677   Huesos hominins. *Nature*, *531*(7595), 504–507. https://doi.org/10.1038/nature17405

678   Mittermeier, Russell A., Louis, Jr., Edward E., Richardson, M., Schwitzer, C., Langrand,

679   O., Rylands, Anthony B., … MacKinnon, K. C. (2010). *Lemurs of Madagascar* (3rd

680   ed.).

681   Pastorini, J., Forstner, M. R. J., & Martin, R. D. (2001). Phylogenetic history of sifakas

682   (*Propithecus*: lemuriformes) derived from mtDNA sequences. *American Journal of*

683   *Primatology*, *53*(1), 1–17. https://doi.org/10.1002/1098-2345(200101)53:1<1::AID-

684   AJP1>3.0.CO;2-J

685   Pearson, R. G. (2015). Asian common toads in Madagascar: An urgent effort to inform

686   surveys and eradication efforts. *Global Change Biology*, *21*(1), 9.

687   https://doi.org/10.1111/gcb.12693

688   Petter, J. J., & Peyrieras, A. (1972). Melanization in the genus *Propithecus* Malagasey

689   lemur. *Journal of Human Evolution*, *1*(4), 379–388. https://doi.org/10.1016/0047-

690   2484(72)90114-5

691   Pfeifer, S. P., Laurent, S., Sousa, V. C., Linnen, C. R., Foll, M., Excoffier, L., … Jensen,

692   J. D. (2018). The evolutionary history of Nebraska deer mice: Local adaptation in

693   the face of strong gene flow. *Molecular Biology and Evolution*, *35*(4), 792–806.

694   https://doi.org/10.1093/molbev/msy004

695   Phillips, S. J., Dudik, M., & Schapire, R. E. (n.d.). Maxent software for modeling species

696   niches and distributions (Version 3.4.1). Retrieved January 3, 2020, from

697   http://biodiversityinformatics.amnh.org/open_source/maxent/

698   Quéméré, E., Crouau-Roy, B., Rabarivola, C., Louis, E. E., & Chikhi, L. (2010).

699   Landscape genetics of an endangered lemur (*Propithecus tattersalli*) within its entire

700   fragmented range. *Molecular Ecology*, *19*(8), 1606–1621.

701   https://doi.org/10.1111/j.1365-294X.2010.04581.x

702   Rakotonirina, H., Kappeler, P. M., & Fichtel, C. (2017). Evolution of facial color pattern

703   complexity in lemurs. *Scientific Reports*, *7*(1), 1–11. https://doi.org/10.1038/s41598-

704   017-15393-7

705   Rumpler, Y., Hauwy, M., Fausser, J. L., Roos, C., Zaramody, A., Andriaholinirina, N., &

706   Zinner, D. (2011). Comparing chromosomal and mitochondrial phylogenies of the

707   Indriidae (Primates, Lemuriformes). *Chromosome Research*, *19*(2), 209–224.

708   https://doi.org/10.1007/s10577-011-9188-5

709   Runemark, A., Hansson, B., Pafilis, P., Valakos, E. D., & Svensson, E. I. (2010). Island

710   biology and morphological divergence of the Skyros wall lizard *Podarcis gaigeae*:

711   A combined role for local selection and genetic drift on color morph frequency

712   divergence? *BMC Evolutionary Biology*, *10*, 296. https://doi.org/10.1186/1471-

713   2148-10-269

714   Sagar, V., Kaelin, C. B., Natesh, M., Reddy, P. A., Mohapatra, R. K., Chhattani, H., …

715   Ramakrishnan, U. (2021). High frequency of an otherwise rare phenotype in a small

716   and isolated tiger population. *Proceedings of the National Academy of Sciences of*

717   *the United States of America*, *118*, 39. https://doi.org/10.1073/pnas.2025273118

718   Salmona, J., Teixeira, H., Rasolondraibe, E., Aleixo-Pais, I., Kun-Rodrigues, C.,

719   Rakotonanahary, A. N., … Chikhi, L. (2015). Genetic diversity, population size, and

720   conservation of the Critically Endangered Perrier's sifaka (*Propithecus perrieri*).

721   *International Journal of Primatology*, *36*(6), 1132–1153.

722   https://doi.org/10.1007/s10764-015-9881-x

723   Santana, S. E., Alfaro, J. L., Noonan, A., & Alfaro, M. E. (2013). Adaptive response to

724   sociality and ecology drives the diversification of facial colour patterns in

725   catarrhines. *Nature Communications*, *4*, 2765. https://doi.org/10.1038/ncomms3765

726   Santana, S. E., Lynch Alfaro, J., & Alfaro, M. E. (2012). Adaptive evolution of facial

727   colour patterns in Neotropical primates. *Proceedings of The Royal Society*

728   *Biological Sciences*, *279*, 2204–2211. https://doi.org/10.1098/rspb.2011.2326

729   Schoener, T. W. (1968). The Anolis lizards of Bimini: Resource partitioning in a

730   complex fauna. *Ecology*, *49*(4), 704–726.

731   Sgarlata, G. M., Salmona, J., Razanaparany, T. P., Rabarivola, C. J., Jan, F.,

732   Rasolondraibe, E., … Bayart, F. (2016). Mitochondrial genetic diversity in the

733   crowned sifaka (*Propithecus coronatus*) in a fragmented landscape. *Primate*

734   *Conservation*, *30*(1), 39–57.

735   Slatkin, M. (1993). Isolation by distance in equilibrium and non-equilibrium populations.

736   *Evolution*, *47*(1), 264–279.

737   Soto-Centeno, J. A., Barrow, L. N., Allen, J. M., & Reed, D. L. (2013). Reevaluation of a

738   classic phylogeographic barrier: New techniques reveal the influence of

739   microgeographic climate variation on population divergence. *Ecology and*

740   *Evolution*, *3*(6), 1603–1613. https://doi.org/10.1002/ece3.576

741   Stevens, M., Stoddard, M. C., & Higham, J. P. (2009). Studying primate color: towards

742   visual system-dependent methods. *International Journal of Primatology*, *30*(6),

743   893–917. https://doi.org/10.1007/s10764-009-9356-z

744   Swets, J. A., & Swets, J. A. (1988). Measuring the accuracy of diagnostic systems.

745   *Science*, *240*(4857), 1285–1293.

746   Tapanes, Elizabeth, Kamilar, Jason M, & Bradley, B. J. (2021). Molecular and cellular

747   processes of pelage growth and pigmentation in primate Evolution. In Pitirri, M.K.,

748   & Richtsmeier, J.T. (Eds.), *Evolutionary cell processes in primates: Genes, skin,*

749   *energetics, breathing, and feeding* (pp. 1–33, Volume 2). CRC Press.

750   Tapanes, E., Jacobs, R. L., Harryman, I., Louis Jr., E. E., Irwin, M. T., Kamilar, J. M., &

751   Bradley, B. J. (2021). Hair phenotype diversity across Indriidae lemurs. *BioRxiv*.

752   https://doi.org/10.1101/2021.10.16.464615

753   Tattersall, I. (1986). Notes on the distribution and taxonomic status of some species of

754   *Propithecus* in Madagascar. *Folia Primatologica*, *46*, 51–63.

755   Vieilledent, G., Cornu, C., Cuní Sanchez, A., Leong Pock-Tsy, J. M., & Danthu, P.

756   (2013). Vulnerability of baobab species to climate change and effectiveness of the

757   protected area network in Madagascar: Towards new conservation priorities.

758   *Biological Conservation*, *166*, 11–22. https://doi.org/10.1016/j.biocon.2013.06.007

759   Warren, D. L., Glor, R. E., & Turelli, M. (2010). ENMTools: A toolbox for comparative

760   studies of environmental niche models. *Ecography*, *33*(3), 607–611.

761   https://doi.org/10.1111/j.1600-0587.2009.06142.x

762   Wheeler, B. C., Bradley, B. J., & Kamilar, J. M. (2011). Predictors of orbital convergence

763   in primates: A test of the snake detection hypothesis of primate evolution. *Journal of*

764   *Human Evolution*, *61*(3), 233–242. https://doi.org/10.1016/j.jhevol.2011.03.007

765   Woolridge, T. B., Kautt, A. F., Lassance, J.-M., McFadden, S., Domingues, V. S.,

766   Mallarino, R., & Hoekstra, H. E. (2021). A novel enhancer of Agouti contributes to

767   parallel evolution of cryptically colored beach mice. *BioRxiv*.

768   https://doi.org/10.1101/2021.11.05.467454

769   Xing, S., Bonebrake, T. C., Tang, C. C., Pickett, E. J., Cheng, W., Greenspan, S. E., …

770   Scheffers, B. R. (2016). Cool habitats support darker and bigger butterflies in

771   Australian tropical forests. *Ecology and Evolution*, *6*(22), 8062–8074.

772   https://doi.org/10.1002/ece3.2464

773   Yeaman, S., & Whitlock, M. C. (2011). The genetic architecture of adaptation under

774   migration-selection balance. *Evolution*, *65*(7), 1897–1911.

775   https://doi.org/10.1111/j.1558-5646.2011.01269.x

776   Zimova, M., Mills, L. S., & Nowak, J. J. (2016). High fitness costs of climate change-

777   induced camouflage mismatch. *Ecology Letters*, *19*(3), 299–307.

778   https://doi.org/10.1111/ele.12568

779

780

781

782

783

784

785

786

787

788

789

790

791

792

793

794

795

796

797

798

799

800 **Figure Legends**

801 **Figure 1** Pelage color variation in diademed sifakas of Tsinjoarivo, Madagascar (a)

802 across the anterior body and (b) across the head

803

804 **Figure 2** A detailed map of the spatial composition of all groups in Tsinjoarivo,

805 Madagascar across three base camps. The yellow circle encompasses Mahatsinjo, the

806 blue circle encompasses Ankadivory, and the grey circle encompasses Vatateza.

807

808 **Figure 3** Scoring schematic use to characterize pelage variation in this study. The scoring

809 chart was adapted from a previous study (Caro et al., 2017). Sifaka illustrations modified

810 with permission, copyright 2013 Stephen D. Nash.

811

812 **Figure 4** A west-east gradient that is formed in Tsinjoarivo, based on 'Precipitation of

813 the Wettest Quarter' and 'Mean Temperature of the Coldest Quarter'

814

815 **Figure 5** Plot of PCA scores representing overall pelage coloration of Tsinjoarivo sifakas

816 across the climate gradient (shown with temperature). Brightness increases with

817 increasing PCA values (and darker sifakas are represented by lower PC values).

818

819 **Figure 6** Plot of PCA scores representing the pelage complexity of Tsinjoarivo sifakas

820 across the climate gradient. Less complex pelage is represented by lower PC values.

821